Reconstructing long-term gully dynamics in Mediterranean agricultural areas

Antonio Hayas[1], Tom Vanwalleghem[1], Ana Laguna[2], Adolfo Peña[3], and Juan V. Giráldez[1,4]

[1]University of Cordoba, Dept. of Agronomy, da Vinci Bldg., Cra Madrid km 396. 14071 Córdoba, Spain
[2]University of Cordoba, Dept. of Applied Physics, Einstein Bldg.
[3]University of Cordoba, Dept. of Rural Engineering, da Vinci Bldg.
[4]Institute for Sustainable Agriculture, CSIC, Dept. of Agronomy, Alameda del Obispo, 14080 Córdoba, Spain
Correspondence to: A. Hayas, z22haloa@uco.es

Abstract. Gully erosion is an important erosive process in Mediterranean basins. However, the long-term dynamics of gully networks and the variations in sediment production in gullies are not well known. Available studies are often conducted only over a few years, while many gully networks form, grow, and change in response to environmental and land use or management changes over a long period. In order to clarify the effect of these changes, it is important to analyze the evolution of the gully network with a high temporal resolution. This study aims at analyzing gully morphodynamics over a long time scale (1956-2013) in a large Mediterranean area in order to quantify gully erosion processes and their contribution to overall sediment dynamics.

A gully network of 20 km^2 located in SW Spain, has been analyzed using a sequence of 10 aerial photographs in the period 1956-2013. The extension of the gully network both increased and decreased in the study period. Gully drainage density varied between 1.93 km km^{-2} in 1956, a minimum of 1.37 km km^{-2} in 1980, and a maximum of 5.40 km km^{-2} in 2013. The main controlling factor of gully activity appeared to be rainfall. Land use changes were found to have only a secondary effect. A new Monte Carlo-based approach was proposed to reconstruct gully erosion rates from orthophotos. Gully erosion rates were found to be relatively stable between 1956 and 2009, with a mean value of 11.2 t ha^{-1}yr^{-1}. In the period 2009-2011, characterized by severe winter rainfalls, this value increased significantly to 591 t ha^{-1}yr^{-1}. These results show that gully erosion rates are highly variable and that a simple interpolation between the starting and ending date greatly underestimate gully contribution during certain years, such as, for example, between 2009 and 2011. This illustrates the importance of the methodology applied using a high temporal resolution of orthophotos.

1 Introduction

Understanding gully erosion dynamics under changing land use and climate conditions is essential for soil and water conservation. Erosion is one of the most significant threats to soils and sustainable agriculture worldwide (Amundson *et al.*, 2015). To satisfy long-term food production and food safety, soil erosion rates should be drastically reduced to the level of soil formation

rates. Additionally, sediment dispersion induces environmental pollution, with severe downstream problems for infrastructure. Soil erosion is a major factor in the anthropogenic perturbation of the global carbon cycle (Regnier *et al.*, 2013). Given its importance, much research effort has gone into characterizing and modelling erosion rates in order to identify key problem areas and propose management solutions. Recently, a European-wide effort was conducted to improve the quantification of

5   water erosion either with RUSLE (Panagos *et al.*, 2015), or with similar models (Quinton *et al.*, 2010; Van Oost *et al.*, 2007). Nevertheless, such models represent a minor part of the water erosion processes by not considering the contribution of gullies. Poesen *et al.* (2002) concluded that gully erosion could be the source of up to 83% of sediment yield in Mediterranean areas. Recent efforts to measure gullies in detail confirm these numbers. For instance Castillo (2012) estimated the range of gully erosion rates in a set of cultivated catchments in Cordoba as being 37 to 250 t $ha^{-1}yr^{-1}$.

10   Most erosion models for gully erosion focus on modelling headcut growth. Examples are REGEM and its adaptation TIEGEM, both used in the model Annualized AGricultural Non-Point Source (AnnAGNPS; Gordon *et al.*, 2007; Taguas *et al.*, 2012), CHILD (Flores-Cervantes *et al.*, 2006; Campo-Bescós *et al.*, 2013) or the headcut growth model by Rengers and Tucker (2014). Kirkby and Bracken (2009) presented an areal gully growth model that showed how the ratio of channel versus sidewall processes is a key determinant in its evolution. In contrast, Dabney *et al.* (2015) modeled gully erosion rates by shear stress by

15   inserting a new Ephemeral Gully Erosion Estimator (EphGEE), included in a new version of RUSLE2, in a small agricultural watershed in Iowa. More mathematically based models seek general laws controlling areal gully growth and ramification (*e.g.* Devauchelle *et al.* 2012). In general however, there is an important lack in suitable field data for understanding and modelling long-term gully evolution.

Different methodologies, apart from traditional field measurements with total station, laser profilemeters and poles (Castillo

20   *et al.*, 2012), have been proposed and successfully applied to estimate gully volumes. For instance, at the individual gully scale, 3D reconstruction from high resolution aerial photography and digital photogrammetry has been widely applied (e.g. Marzolff and Poesen, 2009). Recently, terrestrial imagery modelling and Structure from Motion - Multi View Stereo (SfM - MVS) procedures have been used to determine gully volumes (Gómez-Gutiérrez *et al.* 2014; Frankl *et al.*, 2015 and Castillo *et al.*, 2015). Terrestrial LiDAR has been applied to measure rills or gullies at both laboratory and plot scale (Vinci *et al.*,2016;

25   Momm *et al.*, 2011, 2012). Nevertheless, at the catchment scale, the number of studies is limited. At this scale, most studies focus on the areal extension of gully networks, using aerial photos or other remotely sensed imagery. Few studies report gully volumes due to the inherent difficulties of determining depths for the whole gully network. Nachtergaele and Poesen (1999) determined gully length from aerial photos and, by using additional field measurements, they established a mean cross section to calculate volumes of small ephemeral gullies in the Belgian loess belt. Martínez-Casasnovas (2000) mapped and quantified

30   the erosion produced in gully systems of big dimensions by processing multitemporal orthophotograms and DEMs in a GIS for a 25 km^2 catchment located in NE Spain. Frankl *et al.* (2011) used sequential photographs to link long-term gully and river dynamics to environmental change in Northern Ethiopia. More recently, Peter *et al.* (2014) used UAVs and photogrammetric analysis to quantify gully erosion, albeit at a local scale in the Souss Basin (Morocco).

Due to the recent nature of most of these field studies on gully erosion, their temporal coverage is limited to a few years at best. More recent studies usually focus on one specific moment in time, where the gully system is visited and measured once or during a couple of years. This implies that no dynamic behaviour of the gully system can be described adequately and that it is difficult to single out the controlling processes. Growth of gully systems in the Belgian loess belt was shown by Vanwalleghem *et al.* (2005) to be a highly non-linear process, with a rapid initial growth followed by a stabilization phase. Under different climates, where rainfall is less uniform and much more concentrated, such non-linear gully dynamics can be expected to be accentuated. It could therefore happen that a single measurement of a gully volume that has been growing for several decades does not offer a good estimate of yearly growth rates. Gully growth can be expected to be much greater during specific years compared to the long-term mean. Any model efforts will therefore need experimental data collected with a high temporal resolution.

Over such longer time scales, exceeding several decades, few experimental data are available. Over time scales of up to several centuries, different studies indicate that gully erosion is not a new process. In Northern and Central Europe, gullies have been dated between Early Bronze Age and Late Medieval times (Vanwalleghem *et al.*, 2006). In the Western Mediterranean, with a long history of land use, such historical studies are rare however (Dotterweich, 2013). Over the medium term, of several decades, available studies point to an important dynamic of ephemeral gullies, with erosion phases and infilling ones. These can be due to normal tillage operations for small, ephemeral gullies; deliberately done by farmers in case of larger gullies; or during land use change phases, in which farmers erase such topographic features by tillage, as has been supported by field evidence. Gordon *et al.* (2008) showed by simulations using the REGEM model that those erosion and infilling cycles could produce up to double the amount of sediment as when gullies were left to erode naturally. Each infilling phase prepares sediment for the next important storm event. Field data for this time scale are rare and generally come from the analysis of historical aerial photos. Frankl *et al.* (2013) quantified the evolution of a permanent gully network in Ethiopia using long-term historical aerial photos over the period 1963-2010 for an area of 123 km^2. After an initial stability phase, they identified a peak erosion period in 1994, after which the system stabilized again. These results stress the importance of frequent temporal observations. Saxton *et al.* (2012) analyzed multitemporal aerial photographs between 1951 and 2006 to derive historical gully erosion rates in terms of surface growth per year in three catchments in south-east Queensland in Australia. They associated the gully initiation to post-European settlement land use practice and above average rainfall and runoff. Also, Shellberg *et al.* (2016) observed an increase in the gully erosion by the changes in the land use produced by post-European settlement in the Mitchell River fluvial megafan (Queensland, Australia). This relationship between pioneers and gully erosion was previously suggested by Leopold (1924) in the US. Other methods have been tested, such as using local farmer knowledge on gully morphology (Nyssen *et al.*, 2006; Tebebu *et al.*, 2010) or multi-temporal oblique photography of gully cross sections (Frankl *et al.*, 2011), but the uncertainty in the results is generally too great to allow a quantitative analysis of controlling climate or land use factors.

The objective of this study wass, then, to quantify the erosion and infilling dynamics of a gully network in a typical agricultural area of SW Spain, from historical air photos between 1956 and 2013. A new method is presented that not only allows one to

determine the evolution of gully length, but also, by using Monte Carlo analysis to generate gully width and depth, to calculate the volume of gully erosion and infilling and to constrain uncertainty. Moreover, the controls in terms of land use and rainfall variability are analyzed and the importance of these results for the regional sediment budget assessed.

2 Materials and methods

2.1 Study site

The study area is located between 37.74 and 37.81° N, 4.36 and 4.43° W, in the West Campiña of the Guadalquivir basin in the SW Spain (Fig. 1) and comprises an area of 20.6 km^2. The studied gully network drains towards a series of small ephemeral rivers (Arroyo de Garuñana, Arroyo del Cuadrado, Arroyo del Pozo Muerto, Arroyo de las Monjas, and Arroyo del Barranco), which all drain to the Guadajoz, a tributary of the Guadalquivir river. Although the limits between rills, gullies and larger ephemeral river channels are subject to discussion in the scientific community, this ephemeral river network was not included in the analysis, as it is indicated on the topographical maps and assumed to be stable. The observed gullies can be considered to be mostly permanent (Fig. 2), although some ephemeral ones are included as long as they have a width equal to or higher than the resolution of the orthophotos that were used, ranging between 0.5 and 1.0 m (Table 1).

Gentle hills prevail in the study area except for the south and the center east where steeper ones exist (up to 32%). Altitudes range from 233 to 558 m high and mean slopes are 13%. The soils in the area are dominated by Vertisols, formed mainly in marls and calcareous sandstones deposited during the Miopliocene.

Currently the dominating land uses are olive orchards and herbaceous crops covering almost the whole area, except some 5% of the surface area occupied by grassland. Mean annual precipitation varies between 500 and 600 mm (Córdoba Airport station and Baena RIA station). The distribution of the precipitation shows a marked dry season between June and September, while the main wet period occurs from October to May.

2.2 Rainfall characterization

Characterization of the rainfall regime was performed from daily rainfall collected in the periods 1956-2013 at Castro del Río weather station (37.69° N, 4.47° W), belonging to the Spanish National Meteorological Agency (AEMET). Isolated data gaps of between 1970 and 1971 were filled from the data recorded at Cañete de las Torres weather station (37.83° N, 4.36° W, Phytosanitary Warnings Network of Andalusia, RAIF) and Córdoba Airport weather station (37.84° N 4.84° W, AEMET). Anomalies in annual rainfall were evaluated by means of normalization, through average and standard deviation of annual rainfall for a 57 years period (1956-2013), following Martínez-Casasnovas *et al.* (2003). Values falling outside the interval R_{mean} (average rainfall) $\pm\ sd$ (standard deviation), which correspond to the normalized values >1 and <-1, were considered as anomalies.

The frequency distribution of daily rainfall above a threshold value of 13 mm was analysed, considering this as the minimum rainfall that produces erosive effects as proposed by Wischmeier and Smith (1978) and Renard *et al.* (1997). In addition, the frequency distribution of records above the average daily rainfall event plus the standard deviation were analyzed as well, assuming that these events represent the extreme rainfall events within the study period.

2.3 Photointerpretation process

Analysis of gully evolution and land use change was conducted by photointerpretation based on a dataset of aerial orthophotos of different years from 1956 to 2013. Performance characteristics of the orthophotos dataset are summarized in Table 1. The working scale in the photointerpretation processes was established at 1:5000 for the whole dataset.

2.3.1 Land use

Land use in the study area for 2001, 2005, 2009, 2011, and 2013 was derived from the respective orthophotos while for the rest of the years (1956, 1980, 1984, 1999, 2003, and 2007) existing Maps of the Land Use and Vegetation Cover of Andalusia (Red de Información Ambiental de Andalucía, REDIAM) were employed. Different land uses present in the area were simplified to three classes as shown in Table 2.

2.3.2 Gully network length

Gully length was obtained by digitizing the extension of the network for each available year (Fig. 3), distinguishing between newly incised and infilling stretches. Gully network was decomposed in m_y segments, where subscript y indicates the year. Each segment comprises the length between consecutive junctions (Fig. 4). Due to changes in the drainage network during the study period, the number of segments ranged between 108 in 1980 and 940 in 2013. The total length of the drainage network for a given year, L_y, was calculated as the sum of the lengths of individual segments, $l_{y,i}$

$$L_y = \sum_{i=1}^{m_y} l_{y,i} \tag{1}$$

with m_y equal to the total number of individual segments of the gully network for each digitalized year.

2.3.3 Gully network width

In order to measure gully width representatively 35 stretches were selected from the earliest digitalized gully network of 1956 (Fig. 1), covering a wide range of widths. Gully width was measured at the same locations on later orthophotos, allowing the evaluation of the widening process during the complete study period.

2.4 Field campaign

During 2013 and 2014, several field campaigns were conducted to measure current gully widths and depths with measuring tape and a clinometer (Suunto PM-5/360 PC). Gully top width and depth were measured at 27 representative sections that were located as close as possible to the 35 sections used in the photointerpretation. These representative sections covered the entire range of width and depth variability, including different landscape positions, from upstream close to the divide to the junction with the stream network, and both in gullies on herbaceous crops and under olive trees. This method of combining photointerpretation with field measurements of gully morphology is similar to Nachtergaele and Poesen (1999).

2.5 Monte Carlo-based simulations

Although gully length for the different years between 1956 and 2013 could be determined directly from observations using the available air photographs, determination of the gully volume was not so straightforward. As we used freely available orthophotos, it was only possible to measure the size of the gullies in two dimensions and no measure of depth was readily available. Also observations of gully width for each year were limited to the representative sections measured on the orthophotos of that particular year, and therefore included a term of uncertainty as the real population mean remained unknown.

Estimation of overall gully network volume for each year, $\bar{V}_y$, was therefore tackled by conducting a Monte Carlo simulation in which a volume and an associated uncertainty were calculated for every single gully segment, $l_{y,i}$, described in paragraph 2.3.2 (Fig. 4).

For each year, y, a set of $n = 1000$ estimated cross area sections, $S_{y,i} = \{s_{y,i,j}, j = 1,...,n\}$ for every single segment, $l_{y,i}$, were generated as shown in Figure 5, which required the generation of sets of width and depth values for each year. Each generated section is calculated as

$$s_{y,i,j} = k w_{y,i,j} d_{y,i,j} \tag{2}$$

where k is a shape factor, and $w_{y,i,j}$, and $d_{y,i,j}$, the simulated gully width and depth respectively. Field observations suggested that a triangular section is a reasonable approximation of most gully sections, so a shape factor $k = 0.5$ was adopted in order to compute the simulated sections.

To generate a representative measure of gully width, first of all, the gully width distribution measured for each year by photointerpretation at the representative sections was fitted to different probability distribution functions (normal or Gaussian, gamma, lognormal, exponential and Weibull) using the maximum likelihood method. Next, goodness of fit was evaluated for these different distributions by means of the Kolmogorov-Smirnov statistics. Finally, the best overall fitting theoretical probability distribution was selected to obtain the necessary parameters (μ_y, σ_y) to generate n random simulations of representative gully widths for any particular year.

The estimation of gully depth for each year was based on the field data gathered in 2013-14. In order to estimate depth for

previous years, firstly a width-depth relationship was estimated by linear regression analysis from the collected field data. Such a relationship could only be established for the present-day situation. Uncertainty on this linear width-depth relation was then taken into account by computing the estimated intercept, slope and their respective standard deviations (a, b, s_a, s_b). Assuming a normal distribution, a set of one thousand slope and intercept pairs were simulated. Depths for unique segments $(D_{y,i})$ were then derived from simulated widths and slope-intercept pairs.

Finally, a set of n simulated volumes $V_{y,i} = \{v_{y,i,j}, j = 1, ..., n\}$ was calculated for each year and segment multiplying individual measured lengths by the simulated sections (Fig. 5)

$$v_{y,i,j} = s_{y,i,j} l_{y,i} \tag{3}$$

A set of n different simulated volumes of the complete gully network for a particular year V_y was eventually calculated as the sum of volumes of single segments $v_{y,i,j}$

$$V_y = \{v_{y,i,j}, j = 1, ..., n\} \tag{4}$$

and

$$v_{y,j} = \sum_{i=1}^{m_y} v_{y,i,j} \tag{5}$$

Finally average volume of the total gully network for a given year, $\bar{V}_y$, was computed as

$$\bar{V}_y = \frac{1}{n} \sum_{j=1}^{n} v_{y,j} \tag{6}$$

Erosion rates were then obtained from the difference between pairs of simulated volumes on consecutive dates divided by the duration of the period.

3 Results

3.1 Rainfall characteristics during the study period

The annual rainfall depths in the analysed period ranged between 180 mm in the hydrological years 2004/2005 and 973 mm in 2009/2010, with an average value of 546 mm (Table 3). Figure 6 shows standardized annual rainfall between 1956 and 2013 and the anomalies of annual rainfall. Annual rainfalls over the 0.75 percentile (656 mm) were recorded on 15 occasions of which 10 surpassed the average annual rainfall plus the standard deviation (748 mm). Among the lapses between aerial orthophotos dataset, the period 1984-1999 and 2009-2011 concentrated the highest number of positive extreme annual rainfall events. In 1984-1999 eight out of fifteen records were over the 0.75 percentile, and 6 of them were considered to be anomalies

since they were higher than the average annual rainfall plus the standard deviation. In the period 2009-2011, in both years, larger amounts of annual rainfall than the standard deviation were recorded and can thus be considered anomalous severe rainy period.

Figure 7 shows the distribution of the 3698 daily rainfall events recorded during the study period. Daily rainfall events (R_{24}) higher than 13 mm accounted for 21.7% of the total recorded. Among the different periods the highest proportion of $R_{24} > 13$ mm was recorded in 2009-2011 (27.5 events per year, Table 3) whereas the average proportion was 13.9 R_{24} events>13 mm per year. Rain depths higher than the average value (8.4 mm) plus the standard deviation (10.8 mm) were considered extraordinary events, which were concentrated in a higher proportion in the periods 1984-1999 (10.5 records per year) and 2009-2011 (13 records per year) (Table 3). Maximum daily rainfalls were recorded in the hydrological years 1997/1998 (140 mm) and 2007/2008 (126 mm), with an average value of 48.68 mm for the entire period.

3.2 Land use change

Land use experienced a progressive conversion from herbaceous crops to olive orchards as shown in Figure 8. In the study period, olive orchards grew from 13% to 63% of the total catchment area at the same as time herbaceous crops decreased from 85% to 35% of the total catchment area. The main land use change occurred between 1984 and 1999, when the olive orchards went from occupying 25% to 48% of the total catchment area. The highest rates of change however were observed in the period 2005-2007 with a more than 4% rate of annual land use change from herbaceous crop to olive orchards.

3.3 Gully network length dynamics

Figure 9 shows the evolution of the gully network derived by photo-interpretation between 1956 and 2013, with drainage density included. From 1956 to 2013 the gully network increased not only in length but in number of branches as well. Further analysis on the length and area ratio showed that the drainage density had grown from 17.2 m ha^{-1} to 53.3 m ha^{-1}. There seeems to be a greater increase in the south compared to the north, which suggests a more stable condition in the latter. In most of the analyzed period, the variations in drainage density were small. However, there were two significant periods when the increase was very high and that account for the main increases in the overall value. From 1984 to 1999 and 2009 to 2011 there was an increment of 14.6 m ha^{-1} and 23.6 m ha^{-1}, respectively, which accounted for 84% of the total drainage density growth. When comparing these gully length dynamics to controlling factors of land use and rainfall, it can be seen in Table 3 that this rapid growth could be related to extreme rainfall events that occurred in 1997 and anomalous rainy periods in 2009-2011. In contrast, in some periods, such as for instance in 1956-1980, 1999-2001, 2001-2005 and 2007-2009 the gully network underwent several decreases in the drainage density, although in no case was this decrease more than 4 m ha^{-1}, and can therefore be considered modest. These decreases may be directly related to farming operations, in which farmers fill in the upstream gully stretches that are limited in depth and can be considered to be ephemeral gullies.

Figure 10 shows the frequency distribution of headcut growth and infilling of individual gullies for the different periods between 1956-2013. Some of the observation periods exhibit a balance between infilling and growing reaches, which leads to a very minor overall change of the total gully network length. During a few distinct intervals however, 1984-1999 and 2009-2011, this balance shifts drastically and results in a fast increase of the gully network's total length, as can be seen in Figure 11. This can partly be explained by the fact that, in these two periods infillings are almost negligible (Fig. 10 and Fig. 11). However, in Figure 11, the growth of the gully at the end of those periods (1999 and 2011) is much greater (31 km and 49 km) than those from the other end periods (13 km as the highest value), which clearly shows that gully growth was the dominant process controlling gully dynamics in those periods.

Figure 11 shows how the total length of the gully network tripled from 35.4 km in 1956 to 109.8 km in 2013 (Fig 11). Main enlargement periods were registered in 1980-1984 (10.6 km), 1984-1999 (29.9 km) and 2009-2011 (48.8 km). In contrast, during some other periods, like, for instance, in 1956-1980, 1999-2001, 2001-2005 and 2007-2009, the balance between infilling and growing stretches resulted in a net reduction of the total gully network length. Infilling gully stretches identified during photointerpretation, could be classified into two different types: those made during regular tilling operations at the end of the summer, usually in the order of several tens of meters and those resulting from land levelling during land use change phases, which may reach some hundreds of meters.

Extraordinary annual rainfalls as well as individual extreme precipitation events seem to be the main factors that can be linked to gully retreat (Table 3). Land use does not seem to be the dominant factor controlling these observed peaks in gully length increase. However, we cannot exclude that land use change could have contributed to the rainfall extremes inducing high peak discharges, because, since 1956, a shift from cereal crops to olive orchards occurred in half of the study area, and was especially intensive from 1984 onward. Young olive trees with limited root systems and small canopies leave an important soil surface bare and give little protection to overland flow or gully headcut advance. However, further analysis should be made in order to confirm this hypothesis.

3.4 Gully network width dynamics

Top width at the representative cross sections, as derived from the orthophotos dataset, experienced continuous widening over time (Fig. 12). While at the beginning of the study period (1956), the maximum top width was close to 12.0 m, this value progressively increased over subsequent years, until reaching a maximum value of 59.0 m in 2013. The average value increased smoothly from 4.5 m wide in 1956 to 8.0 m in 2005, whereas the rate of increase for the period 2005-2013 clearly got steeper, resulting in final average width of 13.1 m in 2013. Although widening could be expected at every time step, average widths derived from the cross sections in 2007 (7.7 m) actually experienced a narrowing with respect to those measured in 2005 (8.0 m). Since this period (2005-2007) underwent the highest rate of land use change in the series, this reduction in cross section could be explained by the reopening of gullies that had previously been removed by land leveling during a land use shift to olive orchards.

Table 4 summarizes p-values obtained by means of the Kolmogorov-Smirnov statistic, which was used to evaluate the suitability of different theoretical probability distributions for fitting the observed top widths. The lognormal distribution showed itself to be the most suitable for almost all the years, with the highest p-value of 0.98, in 1980 and 1999 and lowest p-value of 0.64 for 2011, although it was still the best fit for all the distributions tested. These fitted probability distributions were then used to simulate 1000 random widths for each year and single segment composing the gully network.

3.5 Width and Depth relationship

In order to compute the volume of the gully network, depths at the different stretches were derived from the Monte Carlo simulated widths using a width-depth relation resulting from field work, shown in Figure 13. A coefficient of determination $R^2 = 0.83$ was obtained from a logarithm-based fitting, with slope, intercept and their standard deviation, respectively, 1.73 ± 0.16 and 0.55 ± 0.32. Normal deviates based on those coefficients were used to generate 1000 width and depth pairs.

3.6 Gully volume dynamics

Figure 14 presents the final volume evolution, as calculated by means of the Monte Carlo simulation. Gully stretches with a single, observed length were multiplied by the generated width and depth pairs, resulting in 1000 simulated gully network volumes for each stretch and for each period. Average volume in addition to minimum and maximum volumes were then obtained from the set of simulations, showing the growth of the gully in terms of mean eroded volume, as well as a measure of uncertainty, by means of the 5-95% confidence interval of these inferences, shown in grey. Gully network volume grew from 0.18 hm^3 in 1956 to 3.24 hm^3 in 2013. These results show how the original value of the total gully volume has increased 17 times. Main periods of rapid volume growth occurred at the end of the study period, between 2009 and 2013, when the gully volume increased from 0.82 hm^3 until its final value of 3.24 hm^3. Moreover, the period 2009-2011 alone accounts for nearly 52% of the observed growth. Infilling phases were also reflected in the volume evolution curve shown in Figure 14, such as for instance at the end of the period 1956-1980, when the gully volume decreased until it reached its minimum value (0.15 hm^3), and in 2007 which shows a 0.015 hm^3 decrease from the average volume in 2005 (0.81 hm^3).

3.7 Gully erosion rate dynamics

Dynamics of gully erosion rate are shown in Figure 15. Maximum erosion rate was reached in the period 2009-2011 when 591 t ha^{-1}yr^{-1} were lost according to the Monte Carlo results. Minimum erosion rate (-5.21 t ha^{-1}yr^{-1}) was recorded in the period 2005-2007. Negative values here reflect the decrease of the gully network volume, and it should therefore be considered as an infilling not an erosion rate. Average erosion rate for the whole study period was 39.7 t ha^{-1}yr^{-1}.

4 Discussion

The average gully erosion rate of 39.7 t ha^{-1}yr^{-1} for the total catchment area obtained in this study, by means of photo-interpretation techniques combined with stochastic methods, is of the same order of magnitude as those found in the literature in Mediterranean basins. Oostwoud Wijdenes *et al.* (2000) reported erosion rates of 1.2 t ha^{-1}yr^{-1} in bank gullies developing into highly erodible sedimentary deposits in the southeast of Spain, derived by aerial photo analysis over a 38 year period. The highest gully erosion rate of 331 t ha^{-1}yr^{-1} referring to its catchment was found by Martínez-Casasnovas *et al.* (2003) in large gullies in the NE Spain, from high resolution DEMs and GIS analysis in a 36 year period. Compared to other erosion processes, the gully erosion rates measured here almost double the average erosion rates for sheet and rill erosion reported for olive orchards in the Mediterranean (23.2 t ha^{-1}yr^{-1}) by Gómez et al. (2008). Olive orchards are one of the most important crops in the Mediterranean and are generally considered to be highly affected by sheet and rill erosion. This clearly stresses the importance of adequately considering gully erosion processes when modelling soil losses from water erosion.

Most importantly, the results show a wide variability in gully erosion rates, ranging between -5.21 and 591 t ha^{-1}yr^{-1}. This includes periods dominated by infilling and rapid growth, underlining the importance of measuring erosion rates at the finest temporal resolution possible in order to prevent under- and/or overestimations in sediment production. Such variability is in part explained by the inherent irregularity of the local rainfall regime, which appears to be the main controlling factor for gully erosion at this site. However, land use change has played an important role, intensifying in some cases and masking in other cases gully erosion rates. For instance, in the initial period between 1956 and 1980, the erosion rate gave a negative value. However, given the length of this period and since there were some particular years (*i.e.* 1961-1962) with extreme rainfall, it is likely that positive gully growth occurred during this period, that was later masked by infilling. This shows that longer periods, such as 1956-1980 and 1984-1999, were subject to a greater uncertainty with respect to the post-1999 period, when a higher temporal resolution was available. Infilling phases could be expected to be followed by those with higher erosion rates. Gordon *et al.* (2008) obtained the latter from periodically infilled gullies compared to gullies left undisturbed. However, our results do not show that trend. For example, land use change and infilling between 2005 and 2007 was followed by only a moderate gully erosion phase in the 2007-2009 period.

Moreover, the data presented here clearly show that, in Mediterranean areas (Köppen climate type Csa), the gully growth dynamics are different, for instance, to those in Temperate Oceanic west-European areas (Köppen type Cfb). A review of different studies on gully growth over time by Poesen *et al.* (2006) indicated a rapid initial growth, followed by a stable phase with slow growth for "mature" gullies. Data for this study was from the Temperate Oceanic (Cfb) Loess belt or from lab experiments under constant discharge conditions. In our case, with a high variability in natural rainfall, even after several decades, intense growth phases were observed. This observation is not unique since, in another environment Shellberg *et al.* (2016) have detected an almost continuous increasing trend in the gullies of the Mitchell River in Queensland. As stated before, these could mainly be attributed to an increase of the gully's cross sections, and less to a gully headcut retreat. Therefore, models such as

CHILD or REGEM, which have been applied with success to gully modelling, but focus mainly on headcut activities, would probably not yield good results in this case.

From a wider geomorphological perspective, other phenomena such as lowering of the base level and incision of the river bed could be suggested as being a cause of the progressive increase in the erosion rate. During the Quaternary, the main Guadalquivir River was at an incision stage due to its base level fall. However, this incision has been slow, as demonstrated by Uribelarrea and Benito (2008), who found evidence of only a 1.2 m incision over the last 500 years. In any case, since the 1950-60s, when many dams were constructed, the Guadalquivir has been a highly regulated river. Such dams are known to have a downstream incision effect due to removal of sediment load and an upstream aggradation effect. With respect to our study area, there are no upstream but only downstream dams. Therefore, it is surmised that the influence of the incision stage has been artificially limited in this catchment since the 1950s and that the observed changes in the gully network can be fully attributed to upstream changes in the rainfall or land use regimes.

Gully erosion rates computed between the start and the end of the study period would incur in gross underestimation. Erosion rates between 1956 and 2009 were under the average (39.7 t ha^{-1}yr^{-1}), while the last period (2009-2013) accounted for around 52% of the gully volume growth, reaching a peak value of 591 t ha^{-1}yr^{-1} in the period 2009/2011. Nevertheless, these observations are in accordance with other studies in the Mediterranean. Gully erosion rates after some extreme rainfall events in the Mediterranean basin has been reported to occasionally reach 207 t ha^{-1} (Martínez-Casasnovas *et al.*, 2002). In a review of the western Mediterranean basin, González-Hidalgo *et al.* (2007) found that, on average, the three largest daily events per year accounted for more than 50% of the total sediment exported from the basin. Nevertheless Woman and Miller (1960) observed the relevance of relative frequent events of moderate magnitude. Gioia *et al.* (2008) stressed the importance of different runoff thresholds to explain flood occurrence in the Mediterranean areas. Ordinary flows are produced when rainfall rate exceeds the infiltration rate of the soil in a small area, a typical case of Hortonian runoff generation, or Hortonian threshold, while what Gioia *et al.* (2008) denominated outlier events, occurred when the water of almost continuous rain spells surpassed the storage capacity of the soil in a large area of the catchments, or Dunnean threshold. The so-called time compression of Mediterranean climate with respect to soil erosion is therefore very high, as is demonstrated by the data from this study. Our data seem to indicate that land use did not play a dominant role, although we cannot exclude that land use changes to olives and soil management have lowered the land's resilience towards gully incision.

The Monte Carlo stochastic modelling performed allows one to verify that while gully length dynamics (Fig. 11) could explain some of the rapid increases in the volume and erosion rate computed, widening processes (Fig. 12) determine the shape of volume curve (Fig. 14) pointing to the importance of that parameter in the computed volume as opposed, in this particular case, to that suggested by other authors, who, for other areas and climates that the leading controlling parameter is gully length (Nachtergaele and Poesen, 1999). This observation will lead to future field work and modelling efforts, which should not only consider gully headcut advance, but also the mechanisms of gully sidewall collapse and erosion. Possibly a very important factor here, in order to control gully growth, is the possible effect of roots on stabilizing the gully walls (De Baets *et al.*, 2008).

The main advantage of the new method described here, is that by means of Monte Carlo simulation, an estimation of the uncertainty associated with the measurement of gully erosion volume is generated. This is especially relevant when suitable knowledge of erosion dynamics is required, and management systems need to be evaluated or compared. Although more field measurements of gully sections would be advantageous in order to reduce uncertainty, time and money spent on ground

5 truthing would increase accordingly. However, the high p-values of 0.64-0.98 obtained here for the fit between the theoretical probability distribution function and the experimental data suggests satisfactory results can be obtained, even with a limited field sample. Moreover, also Istanbulluoglu *et al.* (2002) successfully used a Monte Carlo approach to estimate gully incision locations using a similar amount of field data.

5 Conclusions

10 A new method was presented to evaluate gully growth over decadal time scales, combining airphotos interpretation with a stochastic approach through Monte Carlo modeling for the channel section parameters. This method constitutes a reliable procedure to determine gully network dynamics over time. Uncertainty ranges obtained in the simulation provide an unprecedented view on the gully network dynamics useful from a management perspective. While highly variable, the observed erosion rates were in accordance with previous studies in Mediterranean basins. The fluctuations in erosion rates were mainly attributed to

15 the variability in rainfall regime variations, likely to have been exacerbated by land use changes, although further research of runoff, gully headcut retreat rates and sidewall dynamics should be made at this last point.

Simple interpolation between the start and end date would highly underestimate gully contribution during certain years, as it could be verified when comparing the average erosion rate (39.7 t ha^{-1}yr^{-1}) with sporadic erosion rates at the end of the study period at to a maximum of 591 t ha^{-1}yr^{-1}. Gully erosion is confirmed to be an important sediment generation process in

20 Mediterranean basins. Average erosion rates from gullies in the study period almost double their values for similar locations and conditions obtained for rill and sheet erosion.

Further studies with more field data are needed to improve the estimations of the contribution of the different land uses to gully growth. Implementation of physically-based models of gully retreat rates and sidewall collapse as well as more field measurements and interviews with local farmers on soil management practice could contribute to a better understanding of the

25 of the elongation processes, and predict gully erosion under different scenarios, including the effect of added root cohesion to sidewall stability or gully headcut protection.

References

Amundson, R., Berhe, A. A., Hopmans, J. W., Olson, C., Sztein, A. E. and Sparks, D. L.: Soil and human security in the 21st century, Science, 348(6235), doi:10.1126/science.1261071, 2015.

Campo-Bescós, M. A., Flores-Cervantes, J. H., Bras, R. L., Casalí, J. and Giráldez, J. V.: Evaluation of a gully headcut retreat model using multitemporal aerial photographs and digital elevation models, J. Geophys. Res. Earth Surf., 118(4), 2012JF002668, doi:10.1002/jgrf.20147, 2013.

Castillo, C.: Metodología de medida de la erosión por cárcavas y modelado de su control mediante diques de retención, Ph.D. diss. University of Córdoba, Dept. of Rural Engineering, http://hdl.handle.net/10396/8521, 2012.

Castillo, C., Pérez, R., James, M.R., Quinton, J.N., Taguas, E.V., and Gómez, J.A.: Comparing the accuracy of several field methods for measuring gully erosion, Soil Sci. Soc. Am. J. 76, 1319-1332, doi:10.2136/sssaj2011.0390, 2012.

Castillo, C., James, M.R., Redel-Macías, M.D., Pérez, R., and Gómez, J.A. 2015. SF3M software: 3-D photo-reconstruction for non-expert users and its application to a gully network, Soil, 1, 583-594, doi:10.5194/soil-1-583-2015, 2015.

Dabney, S., Vieira, D., Yoder, D., Langendoen, E., Wells, R., and Ursic, M.: Spatially distributed sheet, rill, and ephemeral gully Erosion, J. Hydrol. Eng., ASCE, 20(6)C4014009, doi:10.1061/(ASCE)HE.1943-5584.0001120, 2014.

De Baets, S., Poesen, J., Reubens, B., Wemans, K., De Baerdemaeker, J. and Muys, B.: Root tensile strength and root distribution of typical Mediterranean plant species and their contribution to soil shear strength, Pl. Soil, 305(1-2), 207-226, doi:10.1007/s11104-008-9553-0, 2008.

Devauchelle, O., Petroff, A. P., Seybold, H. F. and Rothman, D. H.: Ramification of stream networks, Proc. Natnl. Acad. Sci., 109, 20832-20836, doi:10.1073/pnas.1215218109, 2012.

Dotterweich, M.: The history of human–induced soil erosion: Geomorphic legacies, early descriptions and research, and the development of soil conservation: A global synopsis, Geomorphol., 201, 1-34, doi:10.1016/j.geomorph.2013.07.021, 2013.

Flores-Cervantes, J. H., Istanbulluoglu, E. and Bras, R. L.: Development of gullies on the landscape: A model of headcut retreat resulting from plunge pool erosion, J. Geophys. Res. Earth Surf., 111(F1), F01010, doi:10.1029/2004JF000226, 2006.

Frankl, A., Nyssen, J., De Dapper, M., Haile, M., Deckers, J. and Poesen, J.: Trends in gully erosion as evidenced from repeat photography (North Ethiopia), Landf. Anal., 17, 47-50, 2011.

Frankl, A., Stal, C., Abraha, A., Nyssen, J., Rieke-Zapp, D., De Wulff, A., and Poesen, J.: Detailed recording of gully morphology in 3D through image-based modelling, Catena, 127, 92-101, dx.doi.org/10.1016/j.catena.2014.12.016, 2015.

Gioia, A., Iacobellis, V., Manfreda, S., and Fiorentino, M.: Runoff thresholds in derived flood frequenncy distributions, Hydrol. Earth Syst. Sci., 12, 1295-1307, doi:10.5194/hess-12-1295-2008, 2008.

Gómez, J. A., Giráldez, J. V. and Vanwalleghem, T.: Comments on "Is soil erosion in olive groves as bad as often claimed?" by L. Fleskens and L. Stroosnijder, Geoderma, 147(1-2), 93-95, doi:10.1016/j.geoderma.2008.07.006, 2008.

Gómez-Gutiérrez, A., Schnabel, S., Berenguer-Sempere, F., Lavado-Contador, F., and Rubio-Delgado, J.: Using 3D photo-reconstruction methods to estimate gully headcut erosion, Catena 120, 91-101, doi:10.1016/j.catena.2014.04.004, 2014.

González–Hidalgo, J. C., Peña-Monné, J. L. and de Luis, M.: A review of daily soil erosion in Western Mediterranean areas, CATENA, 71(2), 193-199, doi:10.1016/j.catena.2007.03.005, 2007.

Gordon, L. M., Bennett, S. J., Bingner, R. L., Theurer, F. D. and Alonso, C. V.: Simulating ephemeral gully erosion in AnnAGNPS, Trans. ASABE, 50(3), 857-866, 2007.

Gordon, L. M., Bennett, S. J., Alonso, C. V. and Bingner, R. L.: Modeling long-term soil losses on agricultural fields due to ephemeral gully erosion, J. Soil Water Conserv., 63(4), 173-181, doi:10.2489/jswc.63.4.173, 2008.

5   Hammersley, J.M., and Handscomb, D.C.: Monte Carlo methods, Methuen, London, 1964.

Istanbulluoglu, E., Tarboton, D.G., Park, R.T., and Luce, C.: A probabilistic approach for channel initiation, Water Resour. Res. vol. 38, no. 12, 1325, doi:10.1029/2001WR000782, 2002.

Kirkby, M. J. and Bracken, L. J.: Gully processes and gully dynamics, Earth Surf. Proc. Landf., 34(14), 1841-1851, doi:10.1002/esp.1866, 2009.

10 Leopold, A.: Pioneers and gullies, in Fladder, S.L., and Callicott, J.B. (eds.) The River of the Mother of God and other essays, University of Wisconsin Press, Madison, pp:106-113, 1991.

Martínez-Casanovas, J.A.: A spatial information technology approach for the mapping and quantification of gully erosion. In . Int. Symp. on Gully Erosion under Global Change, Book of Abstracts. K.U. Leuven, Leuven, p. 89, 2000.

Martínez-Casasnovas, J. A., Ramos, M. C. and Ribes-Dasi, M.: Soil erosion caused by extreme rainfall events: mapping and quantification
15 in agricultural plots from very detailed digital elevation models, Geoderma, 105(1), 125-140, 2002.

Martínez-Casasnovas, J. A., Antón-Fernández, C. and Ramos, M. C.: Sediment production in large gullies of the Mediterranean area (NE Spain) from high-resolution digital elevation models and geographical information systems analysis, Earth Surf. Proc. Landf., 28(5), 443-456, doi:10.1002/esp.451, 2003.

Marzolff, I., and Poesen, J.: The potential of 3D gully monitoring withGIS using high?resolution aerial photography and a digital photo-
20 grammetry system, Geomorphol. 111, 48-60, doi:10.1016/j.geomorph.2008.05.047, 2011.

Momm, H.G., Bingner, R.L., Welss, R.R., and Dabney, S.:Methods for gully characterization in agricultural croplands using ground-based light detection and ranging, in Bhuiyan, F. (ed.) Sediment transport - Flow and morphological processes, InTech, ISBN: 978-953-307-374-3, Chap. 5, 2011.

Momm, H.G., Bingner, R.L., Wells, R.R., and Wilcox, D.: AGNPS GIS-based tool for watershed-scale identification and mapping of cropland
25 potential ephemeral gullies, Appl. Eng. Agric. 28, 1-13. 2012.

Nacthergaele, J., and Poesen, J.: Assessment of soil losses by ephemeral gully erosion using high-altitude (stereo) aerial photographs, Earth Surf. Proc. Landf., 24, 693-706, 1999.

Nyssen, J., Poesen, J., Veyret-Picot, M., Moeyersons, J., Haile, M., Deckers, J., Dewit, J., Naudts, J., Teka, K. and Govers, G.: Assessment of gully erosion rates through interviews and measurements: a case study from northern Ethiopia, Earth Surf. Proc. Landf., 31(2), 167-185,
30 doi:10.1002/esp.1317, 2006.

Oostwoud Wijdenes, D. J., Poesen, J., Vandekerckhove, L. and Ghesquiere, M.: Spatial distribution of gully head activity and sediment supply along an ephemeral channel in a Mediterranean environment, Catena, 39(3), 147-167, 2000.

Panagos, P., Borrelli, P., Poesen, J., Ballabio, C., Lugato, E., Meusburger, K., Montanarella, L. and Alewell, C.: The new assessment of soil loss by water erosion in Europe, Environ. Sci. Pol., 54, 438-447, doi:10.1016/j.envsci.2015.08.012, 2015.

Peter, K.D., d'Oleire-Oltmanns, S., Ries, J.B., Marzolff, I., and Hssaine, A.A.: Soil erosion in gully catchments affected by land-levelling measures in the Souss Basin, Morocco, analysed by rainfall simulation and UAV remote sensing data, Catena, 113, 24-40, doi:10.1016/j.catena.2013.09.004, 2014.

Poesen, J., Vandekerckhove, L., Nachtergaele, J., Wijdenes, D. O., Verstraeten, G. and Van Wesemael, B.: Gully erosion in dryland environ-ments, in Bull, L. J. and Kirkby, M. J. (Eds.) Dryland rivers: Hydrology and Geomorphology of semi-arid channels, John Wiley & Son, Chichester, United Kingdom, Chap. 8, 2002.

Poesen, J., Vanwalleghem, T., de Vente, J., Knapen, A., Verstraeten, G. and Martínez-Casasnovas, J. A.: Gully erosion in Europe, in Board-man, J. and Poesen, J. (Eds.), Soil erosion in Europe, John Wiley & Son, Chichester, United Kingdom, Chap. 39, 2006.

Quinton, J. N., Govers, G., Van Oost, K. and Bardgett, R. D.: The impact of agricultural soil erosion on biogeochemical cycling, Nat. Geosci, 3(5), 311-314, doi:10.1038/ngeo838, 2010.

Regnier, P., Friedlingstein, P., Ciais, P., Mackenzie, F. T., Gruber, N., Janssens, I. A., Laruelle, G. G., Lauerwald, R., Luyssaert, S., Andersson, A. J., Arndt, S., Arnosti, C., Borges, A. V., Dale, A. W., Gallego–Sala, A., Godderis, Y., Goossens, N., Hartmann, J., Heinze, C., Ilyina, T., Joos, F., LaRowe, D. E., Leifeld, J., Meysman, F. J. R., Munhoven, G., Raymond, P. A., Spahni, R., Suntharalingam, P. and Thullner, M.: Anthropogenic perturbation of the carbon fluxes from land to ocean, Nat. Geosci, 6(8), 597-607, 2013.

Renard, K. G., Foster, G. R., Weesies, G. A., McCool, D. K. and Yoder, D. C.: Predicting soil erosion by water: a guide to conservation planning with the Revised Universal Soil Loss Equation (RUSLE), USDA Agr. Hbk. 703, USDA, Washington, DC., 1997.

Rengers, F. K. and Tucker, G. E.: Analysis and modeling of gully headcut dynamics, North American high plains, J. Geophys. Res. Earth Surf., 119(5), 983-1003, doi:10.1002/2013JF002962, 2014.

Saxton, N. E., Olley, J. M., Smith, S., Ward, D. P. and Rose, C. W.: Gully erosion in sub–tropical sout-h-east Queensland, Australia, Geo-morphol., 173-174, 80-87, doi:10.1016/j.geomorph.2012.05.030, 2012.

Shellberg, J.G., Spencer, J., Brooks, A.P., and Pietsch, T.J: Degradation of the Mitchell River fluvialmegafan by alluvial gully erosion increased by post-European land use change, Queensland, Australia, Geomorphol., 266, 105-120, doi:/10.1016/j.geomorph.2016.04.021.

Taguas, E. V., Yuan, Y., Bingner, R. L. and Gómez, J. A.: Modeling the contribution of ephemeral gully erosion under differ-ent soil managements: A case study in an olive orchard microcatchment using the AnnAGNPS model, CATENA, 98, 1-16, doi:10.1016/j.catena.2012.06.002, 2012.

Tebebu, T. Y., Abiy, A. Z., Zegeye, A. D., Dahlke, H. E., Easton, Z. M., Tilahun, S. A., Collick, A. S., Kidnau, S., Moges, S., Dadgari, F. and Steenhuis, T. S.: Surface and subsurface flow effect on permanent gully formation and upland erosion near Lake Tana in the northern highlands of Ethiopia, Hydrol. Earth Syst. Sci., 14(11), 2207-2217, doi:10.5194/hess-14-2207-2010, 2010.

Uribelarrea, D., and Benito, G.: Fluvial changes of the Guadalquivir river during the Holocene in Córdoba (Southern Spain), Geomorphol. 100, 14-31, doi:10.1016/j.geomorph.2007.04.037, 2008.

Van Oost, K., Quine, T. A., Govers, G., De Gryze, S., Six, J., Harden, J. W., Ritchie, J. C., McCarty, G. W., Heckrath, G., Kosmas, C., Giráldez, J. V., da Silva, J. R. M. and Merckx, R.: The Impact of Agricultural Soil Erosion on the Global Carbon Cycle, Science, 318(5850), 626629, doi:10.1126/science.1145724, 2007.

Vanwalleghem, T., Bork, H. R., Poesen, J., Schmidtchen, G., Dotterweich, M., Nachtergaele, J., Bork, H., Deckers, J., Brüsch, B., Bungeneers, J. and De Bie, M.: Rapid development and infilling of a buried gully under cropland, central Belgium, CATENA, 63(2-3), 221243, doi:10.1016/j.catena.2005.06.005, 2005.
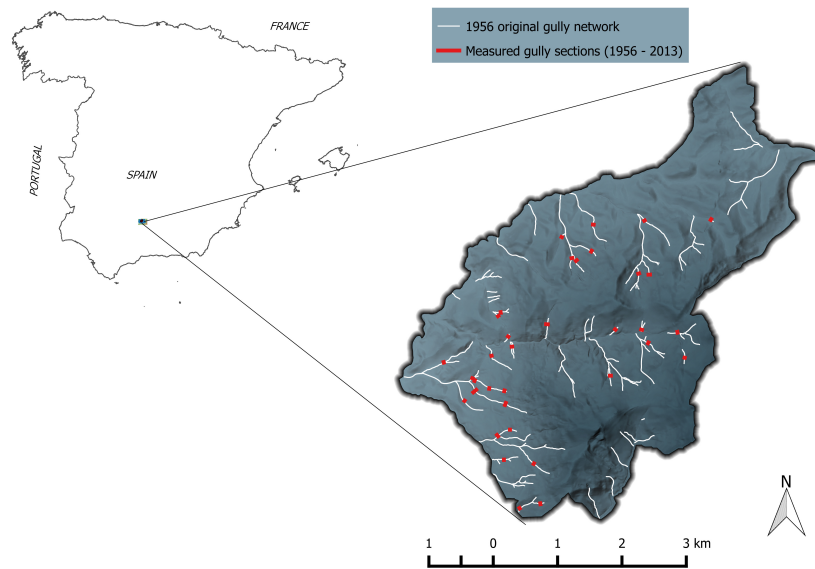
Figure 1. Site location with details of the original gully network and measured gully sections.

Vanwalleghem, T., Bork, H. R., Poesen, J., Dotterweich, M., Schmidtchen, G., Deckers, J., Scheers, S. and Martens, M.: Prehistoric and Roman gullying in the European loess belt: a case study from central Belgium, The Holocene, 16(3), 393-401, doi:10.1191/0959683606hl935rp, 2006.

Vinci, A., Todisco, F., and Mannocchi, F.: Calibration of manual measurements of rills using Terrestrial Laser Scanning, Catena, 140, 164-168, doi:10.1016/j.catena.2016.01.026, 2016.

Wischmeier, W. H. and Smith, D. D.: Predicting rainfall erosion losses-A guide to conservation planning., USDA Ag. Hbk. 537, USDA, Washington D.C., 1978.

Wolman, M. G. and Miller, J. T.: Magnitude and frequency of forces in geomorphic processes, J. Geol. 60, 54-74, 1960.

Figure 2. Typical gullies in olive orchards (left) and in herbaceous crops (right) in the study zone.

Figure 3. Example of orthophotos showing gully incision between 2009 and 2013 from and old (top) into a new plantation (bottom).

Table 1. Orthophoto dataset properties.

capture year	1956	1980	1984	1999	2001	2005	2007	2009	2011	2013
resolution, m	1.0	0.5	1.0	1.0	0.5	0.5	0.5	0.5	0.5	0.5
color	b/w	b/w	b/w	b/w	b/w	col.	col.	col.	col.	col.

b/w: black and white; col.: color

all restitution scales are 1:10,000 except 1980 with scale 1:5,000

$$L_{1956} = \{l_1, l_2, ..., l_m\}$$
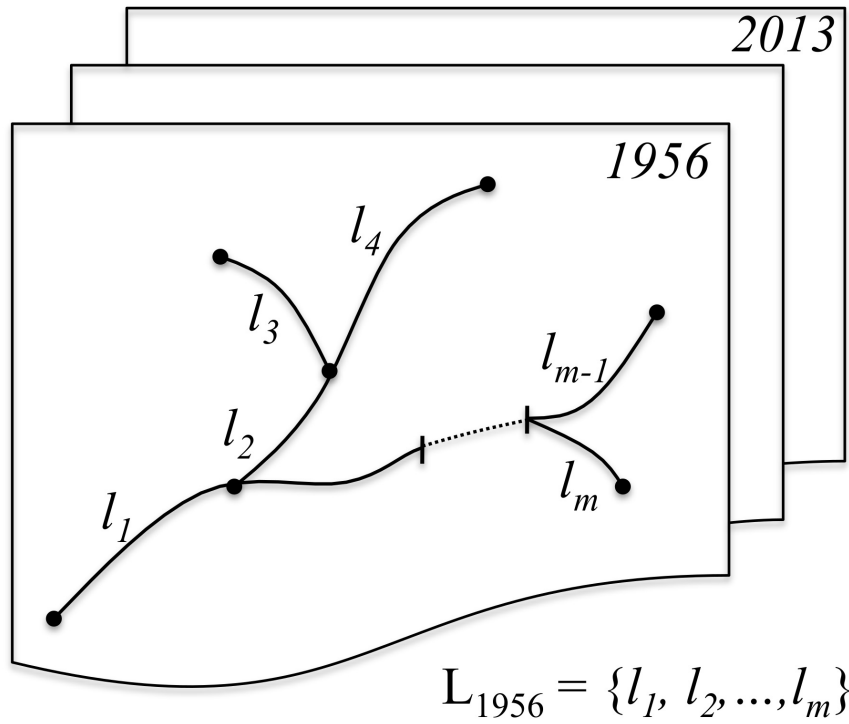
Figure 4. Illustration of the decomposition of the gully network into individual segments for the Monte Carlo-based simulation process.

Table 2. Correspondences of the simplified land use classes adopted in this study with the Map of the Land Use and Vegetation Cover of Andalusia (MUCVA, REDIAM).

MUCVA classes	Simplified classes
Herbaceous crops with scattered trees	
Non-irrigated herbaceous crops	Herbaceous crops
Irrigated herbaceous crops	
Non-irrigated tree crops: olive orchards	Olive orchards
Pasture	
Dense scrubland	Other land use
Streams and natural watercourses	
Agricultural buildings and farms	
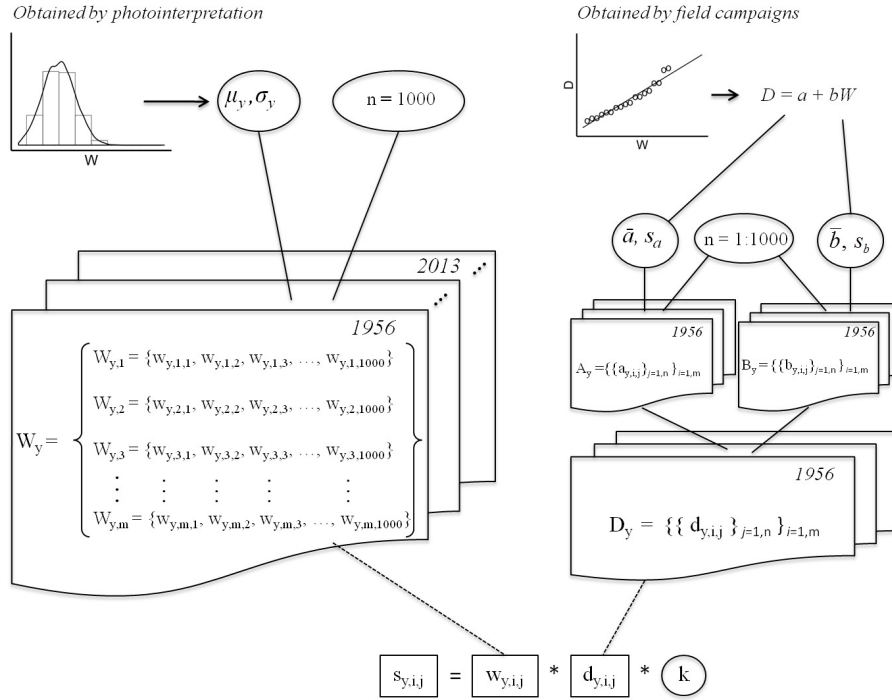
Figure 5. Conceptual scheme of the Monte Carlo simulation processes conducted to generate gully widths ($w_{y,i,j}$: single simulated width for a given segment and year, $W_{y,i}$: set of 1000 simulated widths for a given segment and year) and depths ($d_{y,i,j}$: single simulated depth for a given segment and year, $D_{y,i}$: set of 1000 simulated depths for a given segment and year) and calculate the cross section ($S_{y,i}$) for each gully segment and year. k is a shape factor for the gully cross section, m is the number of gully segment, n is the number of simulations, and a and b are fitted linear regression coefficients of the depth-width relation, with respective means ($\bar{a}, \bar{b}$) and standard deviations (s_a, s_b).
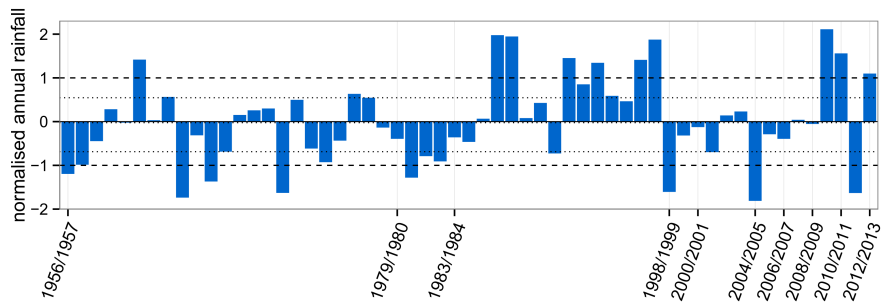
Figure 6. Standardized annual rainfall in the period 1956-2013.
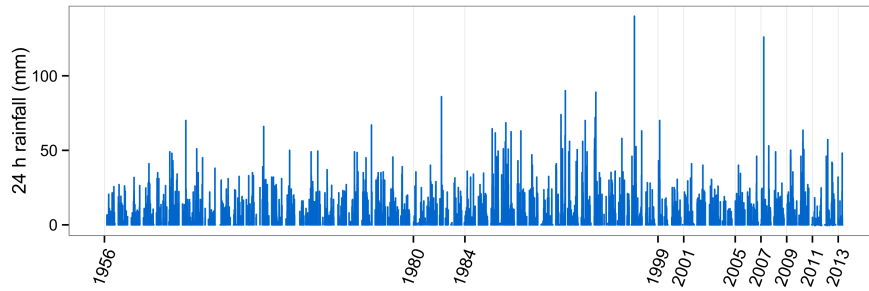
Figure 7. Daily rainfall recorded in the period 1956-2013.
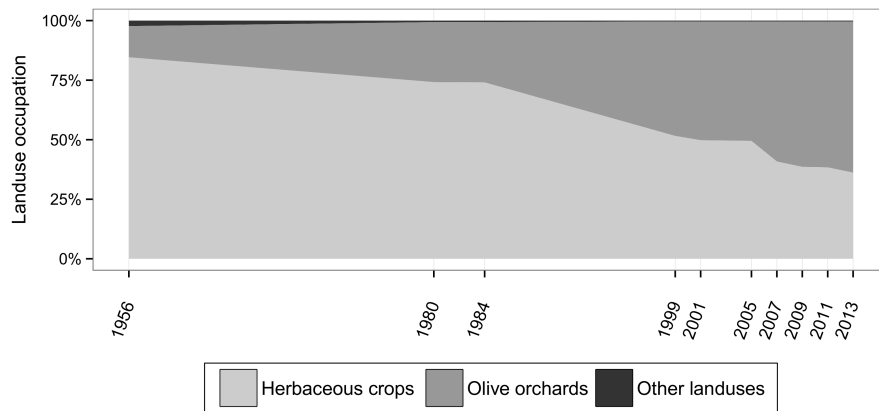
Figure 8. Land use changes in the period 1956-2013.
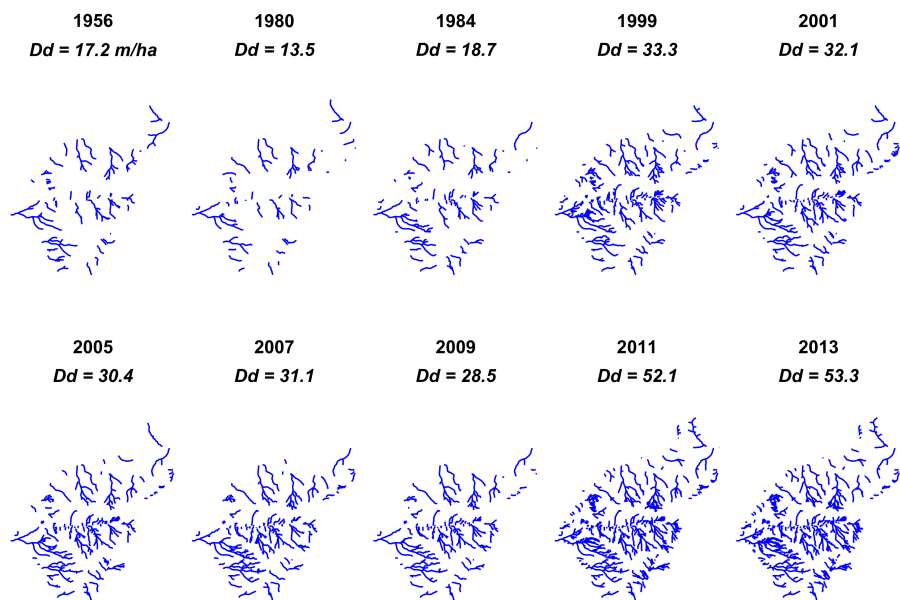
Figure 9. Gully network evolution and drainage density (D_d), in m ha^{-1}, at each period.
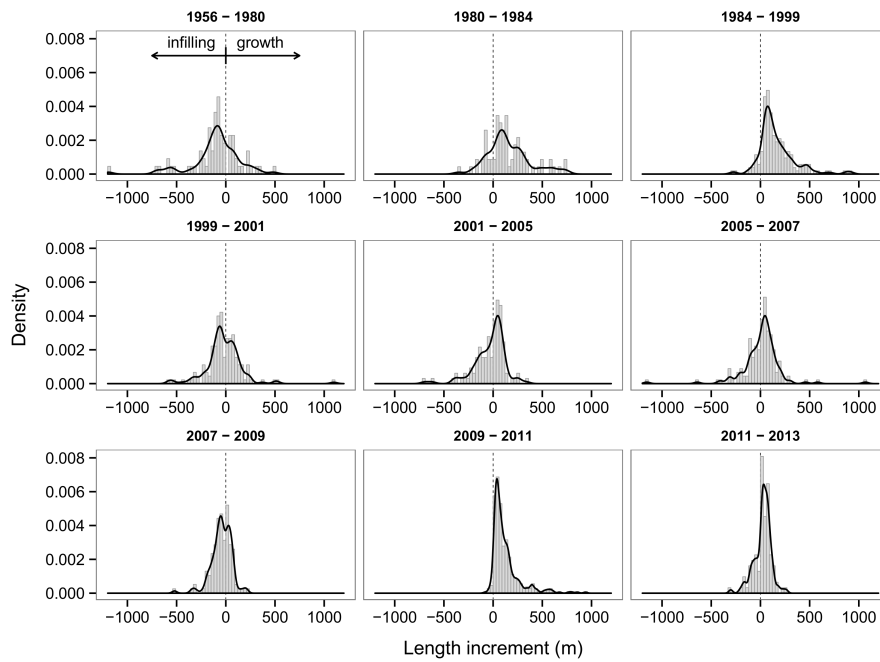
Figure 10. Gully headcut growth or decrease in the different periods between 1956 and 2013.
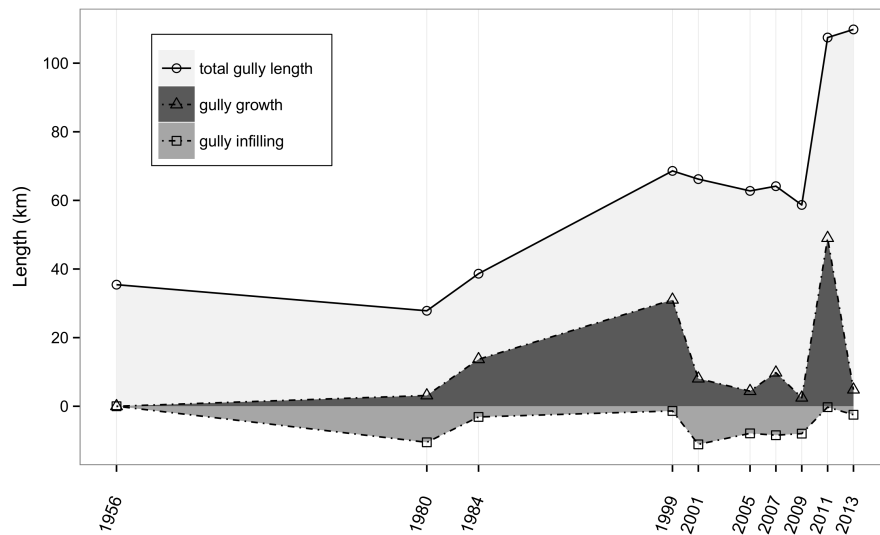
Figure 11. Gully length dynamics in the period 1956-2013.
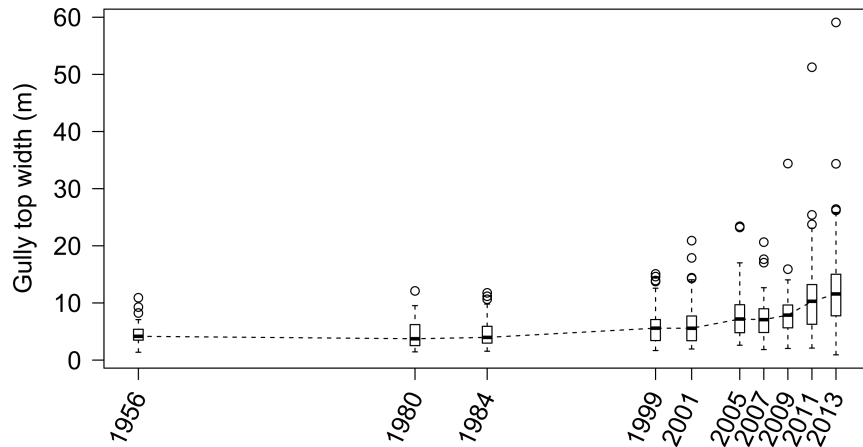
Figure 12. Gully top widths dynamics in the period 1956-2013 derived by measuring by photointerpretation. The dashed line indicates the mean, box and whiskers indicate the 25-50% and 5-95% quantile ranges, respectively.
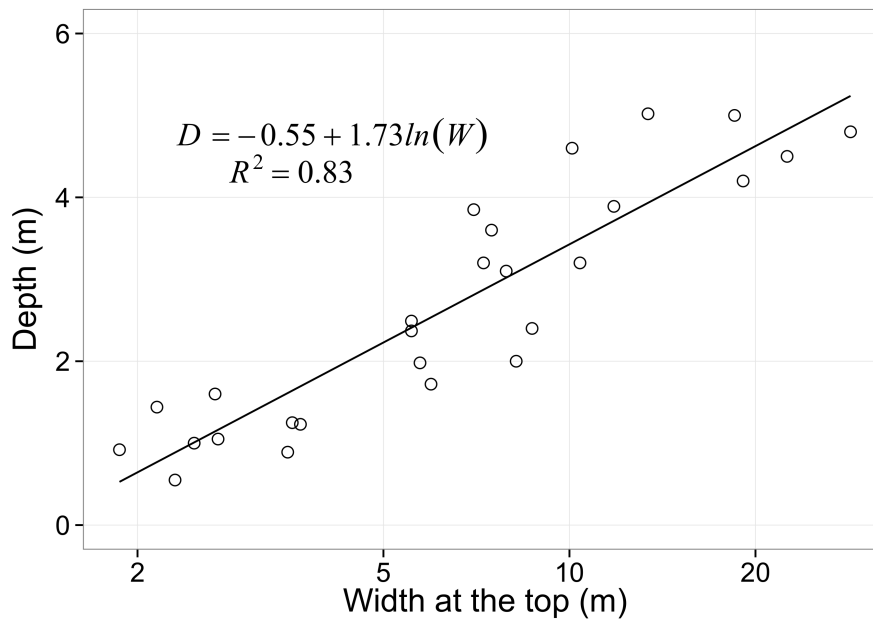
Figure 13. Width-depth relationship derived from field measurements.
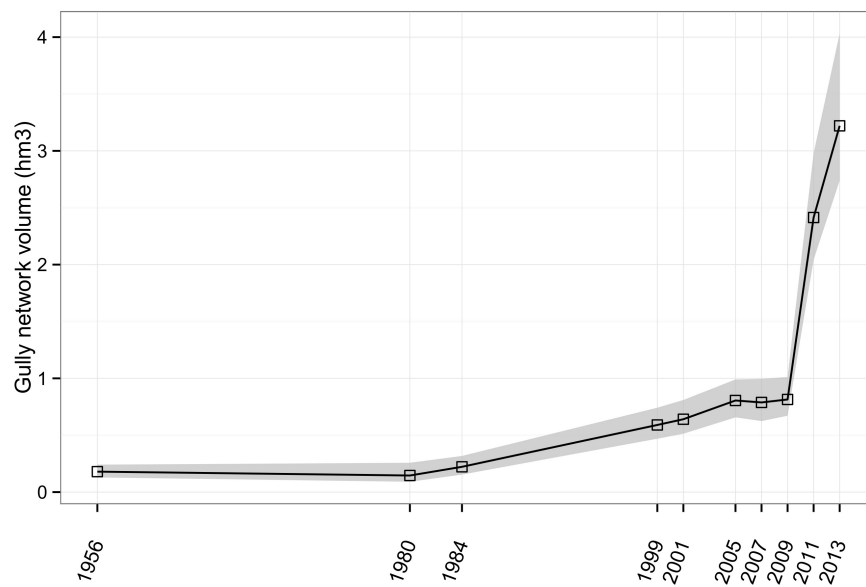
Figure 14. Gully network volume dynamics in the period 1956-2013 and uncertainty interval (grey).
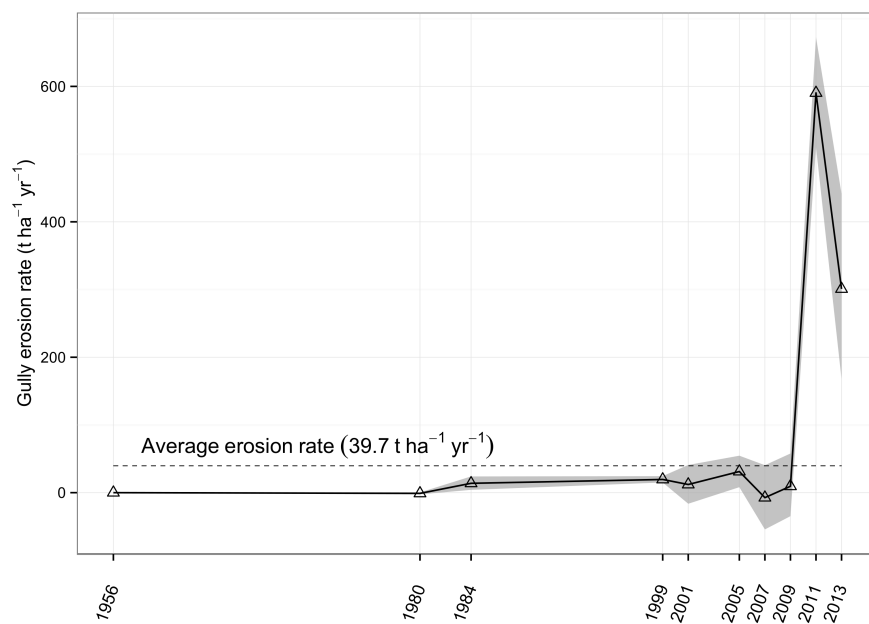
Figure 15. Gully erosion rate in t ha⁻¹yr⁻¹ calculated by Monte Carlo simulation method, and average erosion rate in the period 1956-2013.The grey area represents the 90% uncertainty level

Table 3. Land use, rainfall indicators and gully growth. f_h and f_o: fractions of surface dedicated to herbaceous and olive crops, in the first year of each period. nle: number of 24 hours rainfall events per year higher than 13 mm, $nleo$: number of 24 hours rainfall events per year over the average 24 hours rainfall plus the standard deviation, R_{max}: highest daily rain depth registered within the period, MAR: Mean annual rainfall in the period. ΔL: total, and $\Delta L/\Delta t$, partial increase in gully length, and GH: gully headcut growth, averaged over the area.

period	Δt	land use		rainfall				gully growth		
		f_h	f_o	nle	$nleo$	R_{max}	MAR	ΔL	$\Delta L/\Delta t$	GH
	yr						mm	km	$km\,yr^{-1}$	$m\,ha^{-1}yr^{-1}$
1956		.85	.13							
1956-1980	24	.74	.25	12.9	6.8	70.0	494	-7.37	-0.31	-0.15
1980-1984	4	.74	.25	9.5	5.0	86.0	377	10.58	2.65	1.25
1984-1999	15	.52	.48	17.1	10.5	140.0	677	29.67	1.98	0.94
1999-2001	2	.50	.50	11.0	5.0	70.0	501	-3.06	-1.53	-0.72
2001-2005	4	.49	.50	11.8	4.5	41.0	438	-3.49	-0.87	-0.41
2005-2007	2	.41	.59	13.0	5.5	46.0	477	1.36	0.68	0.32
2007-2009	2	.39	.61	11.5	5.5	126.0	545	-5.48	-2.74	-1.30
2009-2011	2	.38	.61	27.5	13.0	68.5	917	48.77	24.39	11.54
2011-2013	2	.36	.63	12.5	6.0	57.2	492	2.36	1.18	0.56

Table 4. Kolmogorov-Smirnov tests (p-values) obtained by fitting observed gully widths during different years.

pdf	1956	1980	1984	1999	2001	2005	2007	2009	2011	2013
normal	0.18	0.24	0.25	0.19	0.21	0.33	0.21	0.12	0.03	0.07
gamma	0.66	0.77	0.55	0.81	0.74	0.96	0.77	0.67	0.43	0.71
lognormal	0.71	0.98	0.69	0.98	0.97	0.94	0.90	0.92	0.64	0.76
weibull	0.36	0.60	0.60	0.48	0.66	0.65	0.42	0.47	0.21	0.48

pdf: Probability distribution function